Asian Journal of Chemistry; Vol. 37, No. 6 (2025), 1266-1270

ASIAN JOURNAL OF CHEMISTRY

https://doi.org/10.14233/ajchem.2025.33681

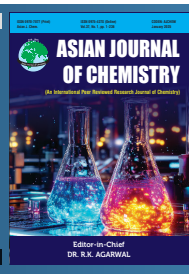

Extracellular Biosynthesis of Ruthenium Oxide Nanoparticles using *Hibiscus sabdariffa* L. and Assessment of Their Biological Activity

AJIT V. DEVALE and AMIT S. VARALE*

Department of Chemistry, A.S.P. College, Devrukh-415804, India

*Corresponding author: E-mail: dspmaspamitdr@gmail.com

Received: 5 March 2025; *Accepted*: 8 April 2025; *Published online*: 27 May 2025; AJC-21996

The present study leverages *Hibiscus sabdariffa* L. as a bio-based platform to develop a green synthesis approach for the fabrication of ruthenium oxide nanoparticles (RuONPs), with a focus on minimizing environmental impact. The extract of *Hibiscus sabdariffa* L. acts as a stabilizing and reducing agent in synthesizing RuONPs. Several techniques *viz*. UV-visible, FT-IR, XRD and SEM were used to clarify the size, shape, crystallinity and surface functional groups in the synthesized RuONPs. The antibacterial, antifungal and antioxidant properties of RuONPs were evaluated as part of the bioactivity assessment.

Keywords: Ruthenium oxide nanoparticles, *Hibiscus sabdariffa* L. Extract, Green nanotechnology, Antibacterial activity.

INTRODUCTION

The distinctive characteristics of nanoscale materials have applications across numerous disciplines, which includes solar cells, chemical sciences, electronics, supercapacitors, batteries, textiles, veterinary medicine, health sciences, *etc*. [1,2]. Previously, efforts emphasized on the synthesis of nanoscale materials by top-down methodologies. Eventually, as a result of its constraints, the bottom-up approach gained popularity. Various researchers have made efforts to synthesize nanoscale materials through bottom-up synthesis methods. Since green method approaches to synthesis are becoming more and more popular, several researchers [3-5] have successfully synthesized transition metal nanoparticles, particularly silver nanoparticles, using plant extracts.

After second world war, antibiotics are widely used for the treatment and control of infectious diseases Penicillin is the first antibiotic extracted from fungus. Although it worked wonders in preliminary tests, however, the infectious microbes eventually developed resistance [6,7]. Thus, there was need to find out certain another antibiotics or material which can combat with pathogenic microorganisms [8,9]. Thus, there is continuous research for the development of antibiotics. It is estimated that if resistance for antibiotics proceeds in such speed then by 2050, all the antibiotics will be ineffective. The antibacterial activity is measured to investigate possible uses in the fight against microbial infections [10,11]. Nanomaterials are new hope for researchers and doctors to have effective antimicrobial activity [12]. The antioxidant properties of the nanoparticles are investigated, highlighting their potential function in scavenging oxidative stress and free radicals [13-15]. This study is an essential addition to the rapidly developing field of green nanotechnology. This work explores the biomedical applications of ruthenium oxide nanoparticles (RuONPs) synthesized from *Hibiscus sabdariffa* L. extract and examines the environmental issues linked to traditional synthesis methods [16,17]. The results are expected to open novel opportunities for applying ruthenium nanoparticles in various biological contexts and pave the way for sustainable nanomaterial synthesis [18,19].

EXPERIMENTAL

Ruthenium trichloride ($RuCl_3$) and the solvents were procured from the commercial source and used without further purification. The fresh leaf of *H. sabdariffa* was collected from the sub-campus Devrukh, (Sangmeshwar) Ratnagiri, India.

Preparation of extract of *H. sabdariffa*: The fresh leaves of *H. sabdariffa* were thoroughly washed several times with tap water and double distilled water and finally dried in the shade at room temperature. A grinder was used to grind the dried leaves into a powder. A 5 g sample of dried leaf powder

was subjected to hydrothermal extraction by boiling 100 mL of double-distilled water at 50-60 ºC for 20 min. The extracted mixture was brought to ambient temperature and then subjected to filtration using Whatman No. 1 filter paper, effectively removing particulate impurities. The obtained filtrate was stored under refrigeration at 5 ºC in a sealed container, designated for subsequent applications. The filtrate is referred to as the S1 extract.

Synthesis of ruthenium oxide nanoparticles (RuONPs): The biosynthesis of RuONPs was initiated by mixing *Hibiscus sabdariffa* leaf extract with 100 mL of 2 mM $RuCl_3$ solution, resulting in the formation of RuONPs. The mixture was stirred at a temperature range of 60-70 ºC for 60 min. Significantly, the reduction of RuONPs was evident within 30 min as indicated by a colorimetric change from brown to a dark yellow-black, signifying the successful formation of RuONPs.

Characterization: An assessment of the optical attributes of the synthesized nanoparticles was conducted by recording their ultraviolet-visible (UV-Vis) absorption spectra with the aid of a JASCO V-770 spectrophotometric analyser. The crystallographic structure and phase purity of the synthesized materials were investigated using XRD analysis using a BRUKER AXS D8 powder diffractometer equipped with Cu*K*α radiation (λ = 0.15425 nm) over a 2θ range of 20-80º. The molecular composition of the synthesized materials was elucidated through the acquisition of their FTIR spectroscopic profiles, which were obtained using a JASCO FTIR-410 spectrometer. The chemical constituents present in the samples were investigated by preparing 1% KBr pellets from the powdered samples and lyophilized plant extract. Morphological characterization and elemental composition analysis of the sample surfaces were performed using scanning electron microscopy (SEM) combined with energy-dispersive X-ray spectroscopy (EDX) on a JEOL JSM-IT200 instrument. Prior to SEM analysis, the powdered samples were deposited onto carbon tape and sputter-coated with gold to enhance conductivity.

Biological activities: The antibacterial efficacy of RuONPs was assessed against selected bacterial strains *viz*. Gram-positive [*Staphylococcus aureus* (NCIM 2654), *Bacillus subtilis* (NCIM 2635) and *Streptococcus pneumoniae* (NCIM 5281)] and Gram-negative [*Escherichia coli* (NCIM 2832), *Klebsiella pneumoniae* (NCIM 2883) and *Pseudomonas aeruginosa* (NCIM 5032)] using a modified agar well diffusion assay [8,9]. Fungal pathogens such as *Aspergillus niger* NCIM 1456 and *Candida albicans* NCIM 3466 were selected for antifungal activity by a modified agar well diffusion method. Antifungal activities were also evaluated using a similar protocol. The MGYP agar plates, comprising malt extract, glucose, yeast extract and peptone, were prepared and inoculated with the respective fungal strain using the immersion inoculation technique [11-12]. The inoculated plates were incubated at a controlled temperature of 27 ºC for 48-72 h. Subsequently, the diameters of the resulting inhibition zones were quantitatively assessed using a calibrated meter ruler. Each experiment was performed in triplicate and the mean value was calculated. The antioxidant properties of the synthesized RuONPs were evaluated using the DPPH (1,1-diphenyl-2-picrylhydrazyl) free radical scavenging assay, a widely recognized method for assessing antioxidant activity [13,14]. A reaction mixture was formulated by mixing 1 mL of RuONPs solution (25-100 µg) with 2 mL of methanolic DPPH radical solution (1.0 mmol L^{-1}). After a 30 min incubation period in dark at 37 ºC, the absorbance was quantified at 517 nm using a Shimadzu UV-1800 spectrophotometer.

RESULTS AND DISCUSSION

UV-visible spectral studies: The optical absorption spectrum were acquired over a broad spectral range spanning 200-800 nm. The appearance of a distinct absorption peak at approximately 275 nm confirmed the formation of ruthenium nanoparticles (Fig. 1).

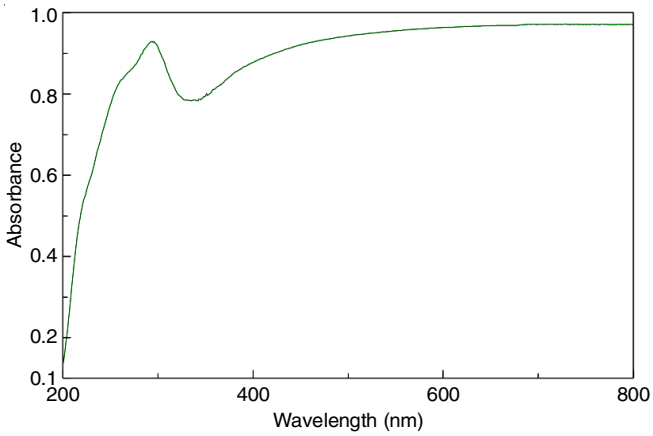

Fig. 1. UV-Vis spectrum of synthesized RuONPs

FT-IR spectral studies: FTIR spectroscopy revealed the presence of characteristic absorption bands corresponding to various functional groups in the aqueous extract of *H. sabdariffa*. (Fig. 2). The IR peak at about 3440 cm^{-1} was due to the –OH stretching of water molecule. The presence of aromatic compounds was characterized by the absorption bands at 2924, 1644, 1513, 1459 and 1392 cm^{-1}. These bands correspond to the vibrational modes of aromatic amines (C=C stretching), aromatic C-H bonds and various C-C and C=C stretching vibrations, including asymmetric C=C-C, symmetric C-C=C and C=C bond stretching, respectively. The infrared spectrum revealed a C-H bending vibration at approximately 817 cm^{-1}. Furthermore, an additional peak at 448 cm^{-1} was observed, which is the characteristic of metallic ruthenium (Ru). It was also observed that $RuCl_3$ reduction to RuONPs may cause the C-H bending peak to rise.

XRD studies: The XRD spectrum of the biogenic RuONPs exhibited distinct peaks at 21.77º, 31.49º, 40.55º, 50.20º, 58.45º and 67.35º, corresponding to the planes (100), (002), (101), (102), (110) and (202), respectively (Fig. 3). The distinctive peaks for RuONPs were also observed in the XRD patterns, indicating the spherical structure of the RuONPs. The average particle size of the RuONPs was calculated using the Debye-Scherrer's equation:

$$D = \frac{K\lambda}{\beta \cos\theta}$$

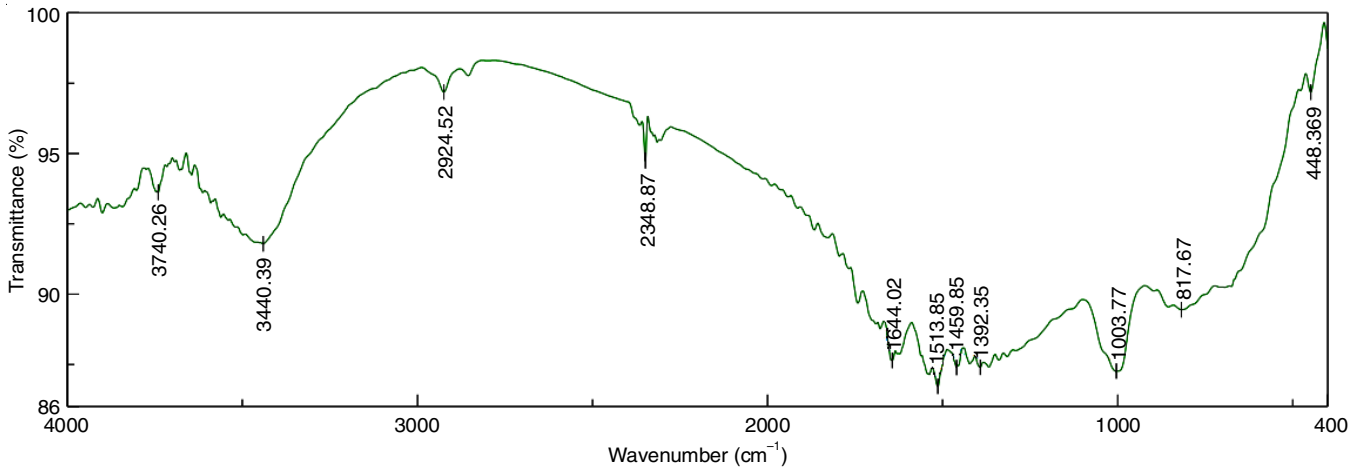

Fig. 2. FT-IR spectrum of synthesized RuONPs

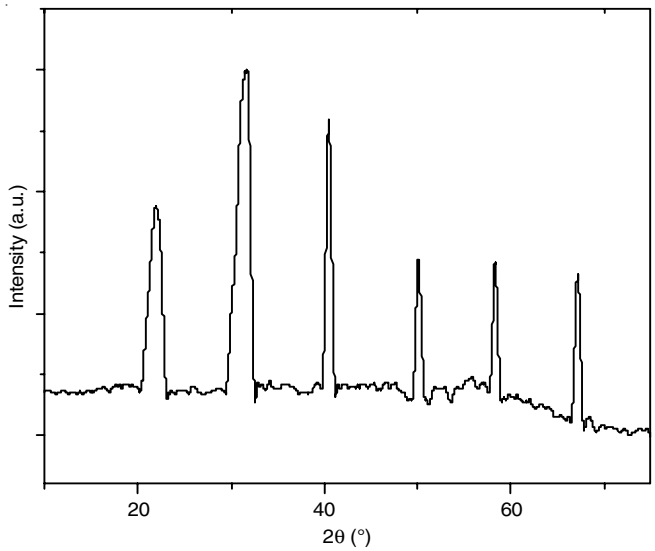

Fig. 3. XRD spectrum of synthesized RuONPs

where D represents the particle size (in nm); K represents the Scherrer constant (0.94); λ is the wavelength of the X-ray source (0.1541 nm); β is the full width at half maximum of the diffraction peak (in radians) and θ is the Bragg's angle. The average crystal size of the RuONPs was found to be less than 50 nm.

SEM-EDX studies: SEM analysis was used to examine the size and surface shape of the green synthesized RuONPs. The RuONPs have an average size of roughly 30 nm and are primarily spherical. The 2,000× (Fig. 4a) and 5,000× (Fig. 4b) magnifications both demonstrated that the nanoparticles are narrowly sized and had spherical shapes. The chemical composition of RuONPs derived from *H. sabdariffa* leaf extract was analyzed by energy-dispersive X-ray spectroscopy (Fig. 4c). The EDX spectrum revealed a distinct peak at 2.6 keV, corresponding to ruthenium (Ru), accompanied by weaker oxygen (O) peaks.

Biological activity

Antibacterial activity: The antibacterial activities of RuO NPs were evaluated against a diverse range of bacterial strains. The assessment was performed using a modified agar well diffusion method. In the antimicrobial assay, the microbial pathogens were inoculated onto sterile Müller-Hinton agar plates and evenly dispersed using a sterile spreader. Subsequently, an agar well was aseptically prepared using a sterilized cork borer measuring 0.7 cm in diameter. The prepared agar plates were then inoculated with 100 µL of the respective sample solution, with concentrations ranging from 25 to 100 µg/mL. To facilitate sample diffusion, the plates underwent a two-stage incubation protocol, commencing with a 20 min refrigeration period at 4

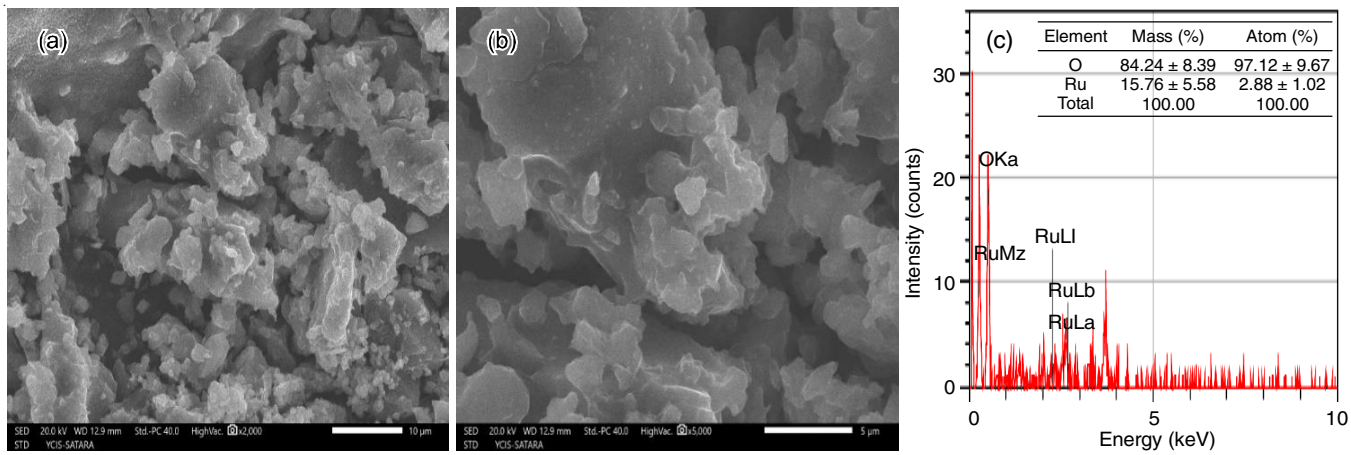

Fig. 4. SEM and EDX images of synthesized RuONPs

ºC to establish a stable pre-incubation environment. This was followed by a 24 h incubation at 37 ºC, optimized for microbial growth and development. The efficacy of the samples was subsequently evaluated by comparing the results with those obtained from the positive control (streptomycin, 1000 µg/mL) and negative control (sterile distilled water) (Table-1).

Ruthenium oxide nanoparticles exhibit antimicrobial efficacy at various concentrations against diverse organisms, demonstrating activity against *S. aureus* at 75 µg/mL, *B. subtilis* at 50 µg/mL and *P. aeruginosa* at 100 µg/mL. Other test species, such as *B. subtilis*, *E. coli* and *K. pneumoniae*, exhibited inferior antibacterial activity relative to streptomycin antibiotic.

Antifungal activities: Fungal pathogens such as *A. niger* NCIM 1456 and *C. albicans* NCIM 3466 were used for antifungal activity by a modified agar well diffusion method. The MGYP agar plates were prepared and inoculated with the respective fungal strains *via* immersion inoculation. After inoculation, the plates were subjected to incubation at 27 ºC for 48-72 h. Subsequent examination revealed the presence of distinct clearance zones surrounding the wells, denoting effective antifungal inhibition. The antifungal efficacy of the tested samples was evaluated by comparing the results with those obtained using ketoconazole (1000 µg/mL), which served as a positive control, while sterile distilled water was kept as a negative control for this study (Table-2). The present study provides information that the RuONPs shows antifungal activity against *C. albicans* at 75 and 100 µg/mL concentrations. In contrast, the RuONPs shows no effect against *A. niger*.

Antioxidant activity: The antioxidant activity of the synthesized RuONPs were assessed using the DPPH radical scavenging assay. A mixture of 1 mL of RuONPs suspensions, spanning concentrations of 25-100 µg/mL and 2 mL of methanolic solution containing 1.0 mmol L^{-1} DPPH radicals, was allowed to react in dark at 37 ºC for 30 min. Subsequently, the absorbance of the resulting solution was quantified at a wavelength of 517 nm using a UV-1800 spectrophotometer. The percentage inhibition of DPPH radicals was determined using the following formula:

$$\text{Radical scavenging activity (\%)} = \frac{\text{Control value} - \text{Sample value}}{\text{Control value}} \times 100$$

The results are illustrated graphically, with ascorbic acid at a concentration of 100 µg/mL used as a reference standard for comparative purposes (Fig. 5).

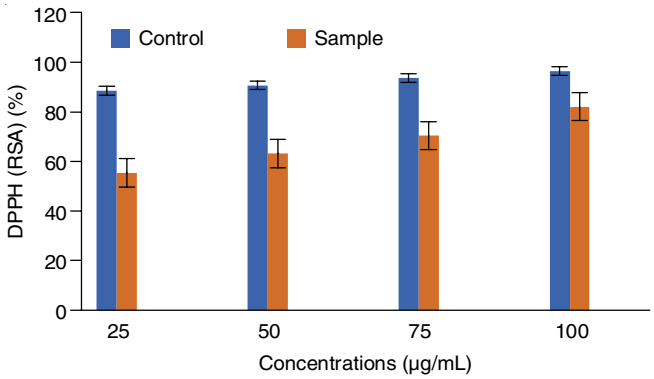

Fig. 5. Antioxidant activity of synthesized RuONPs

The ruthenium oxide nanoparticles exhibited remarkable scavenging activity, with the highest efficacy observed at a concentration of 100 µg/mL, yielding 82.14 ± 0.67% scavenging activity. Notably, the scavenging activity decreased with decreasing nanoparticle concentration, with 75 µg/mL, 50 µg/mL and 25 µg/mL concentrations resulting in 70.36 ± 1.52%, 63.24 ± 1.11% and 55.32 ± 0.71% scavenging activity, respectively.

Conclusion

This study reports the eco-friendly synthesis of ruthenium oxide nanoparticles (RuONPs) using *Hibiscus sabdariffa* leaf extract. The findings demonstrated that plant leaf extracts offer a convenient, cost-effective and environmentally benign method for synthesizing metallic nanoparticles. The structural and compositional properties of the synthesized RuONPs were elucidated using spectroscopic and microscopic techniques, including UV-Vis, FTIR, XRD and SEM. The FTIR spectroscopy indicated

TABLE-1
ZONE OF INHIBITION OF RuONPs AGAINST TEST ORGANISMS

Test organisms	Zone of inhibition (mm)						
	25 µg	50 µg	75 µg	100 µg	Streptomycin (positive control)	DMSO (negative control)	Water (negative control)
S. aureus	00.0	00.0	16.0	22.0	22.0	00.0	00.0
B. subtilis	00.0	15.0	20.0	24.0	24.0	00.0	00.0
S. pneumonia	00.0	00.0	00.0	00.0	21.0	00.0	00.0
E. coli	00.0	00.0	00.0	00.0	26.0	00.0	00.0
K. pneumoniae	00.0	00.0	00.0	00.0	25.0	00.0	00.0
P. aeruginosa	00.0	00.0	00.0	26.0	21.0	00.0	00.0

TABLE-2
ANTIFUNGAL ACTIVITY DATA OF RuONPs AGAINST FUNGAL PATHOGENS

Test organisms	Zone of inhibition (mm)						
	25 µg	50 µg	75 µg	100 µg	Ketoconazole (positive control)	DMSO (negative control)	Water (negative control)
A. niger	00.0	00.0	00.0	00.0	21.0	00.0	00.0
C. albicans	00.0	00.0	21.0	24.0	25.0	00.0	00.0

the presence of several organic compounds in the extracts, which played a crucial role in facilitating the reduction, capping and stabilization of the RuONPs. Furthermore, the RuONPs demonstrated superior antimicrobial efficacy against a panel of microbial pathogens, including *S. aureus*, *B. subtilis* and *P. aeruginosa* surpassing that of the crude leaf extract. The biogenic RuONPs demonstrated promising antifungal properties against *C. albicans*. The green synthesized RuONPs showed increased antioxidant activity and are non-toxic to bacteria, highlighting their potential medical applications.

ACKNOWLEDGEMENTS

The authors appreciate the support and facilities provided by their respective institutions, which facilitated the completion of this work.

CONFLICT OF INTEREST

The authors declare that there is no conflict of interests regarding the publication of this article.

REFERENCES

1. T. Mustapha, N. Misni, N.R. Ithnin, A.M. Daskum and N.Z. Unyah, *Int. J. Environ. Res. Public Health*, **19**, 674 (2022); https://doi.org/10.3390/ijerph19020674
2. J. Singh, T. Dutta, K.H. Kim, M. Rawat, P. Samddar and P. Kumar, *J. Nanobiotechnology*, **16**, 84 (2018); https://doi.org/10.1186/s12951-018-0408-4
3. K. Vijayaraghavan, S.P.K. Nalini, N.U. Prakash and D. Madhankumar, *Colloids Surf. B Biointerfaces*, **94**, 114 (2012); https://doi.org/10.1016/j.colsurfb.2012.01.026
4. M.M.H. Khalil, E.H. Ismail and F. El-Magdoub, *Arab. J. Chem.*, **5**, 431 (2012); https://doi.org/10.1016/j.arabjc.2010.11.011
5. A.W. Alshameri and M. Owais, *OpenNano*, **8**, 100077 (2022); https://doi.org/10.1016/j.onano.2022.100077
6. T.M. Uddin, A.J. Chakraborty, A. Khusro, B.M.R.M. Zidan, S. Mitra, T.B. Emran, K. Dhama, M.K.H. Ripon, M. Gajdács, M.U.K. Sahibzada, M.J. Hossain and N. Koirala, *J. Infect. Public Health*, **14**, 1750 (2021); https://doi.org/10.1016/j.jiph.2021.10.020
7. J.H. Rex, G.H. Talbot, M.J. Goldberger, B.I. Eisenstein, R.M. Echols, J.F. Tomayko, M.N. Dudley and A. Dane, *Clin. Infect. Dis.*, **65**, 141 (2017); https://doi.org/10.1093/cid/cix246
8. B. Regmi, T.R. Binadi, S.N. Jha, R.K. Chaudhary, B.R. Poudel and S.K. Gautam, *Int. J. Appl. Sci. Biotechnol.*, **9**, 220 (2021); https://doi.org/10.3126/ijasbt.v9i3.39069
9. S.D. Deshmukh, S.R. Patil and A.M. Sonkamble, *Int. J. Curr. Microbiol. Appl. Sci.*, **9**, 1132 (2020); https://doi.org/10.20546/ijcmas.2020.906.140
10. K. Gopinath, V. Karthika, S. Gowri, V. Senthilkumar, S. Kumaresan and A. Arumugam, *J. Nanostructure Chem.*, **4**, 83 (2014); https://doi.org/10.1007/s40097-014-0083-4
11. P.M.A.H. Mfengwana and B.T. Sone, *Sci. Rep.*, **13**, 22638 (2023); https://doi.org/10.1038/s41598-023-50005-7
12. W. Wonsawat and Y. Panprom, *Key Eng. Mater.*, **675-676**, 121 (2016); https://doi.org/10.4028/www.scientific.net/KEM.675-676.121
13. S.V. Otari, R.M. Patil, N.H. Nadaf, S.J. Ghosh and S.H. Pawar, *Mater. Lett.*, **72**, 92 (2012); https://doi.org/10.1016/j.matlet.2011.12.109
14. P. Ubale, S. Mokale, S. More, S. Waghamare, V. More, N. Munirathinam, S. Dilipkumar, R.K. Das, S. Reja, V.B. Helavi and S.P. Kollur, *J. Mol. Struct.*, **1251**, 131984 (2022); https://doi.org/10.1016/j.molstruc.2021.131984
15. A. Rangayasami, K. Kannan, S. Joshi and M. Subban, *Biocatal. Agric. Biotechnol.*, **27**, 101690 (2020); https://doi.org/10.1016/j.bcab.2020.101690
16. M. Priya, R. Venkatesan, S. Deepa, S.S. Sana, S. Arumugam, A.M. Karami, A.A. Vetcher and S.C. Kim, *Sci. Rep.*, **13**, 18838 (2023); https://doi.org/10.1038/s41598-023-46002-5
17. S.C. Mali, A. Dhaka, C.K. Githala and R. Trivedi, *Biotechnol. Rep.*, **27**, e00518 (2020); https://doi.org/10.1016/j.btre.2020.e00518
18. A. Arshad, H. Osman, M.C. Bagley, C.K. Lam, S. Mohamad and A.S.M. Zahariluddin, *Eur. J. Med. Chem.*, **46**, 3788 (2011); https://doi.org/10.1016/j.ejmech.2011.05.044
19. R. Gurav, S.K. Surve, S. Babar, P. Choudhari, D. Patil, V. More, S. Sankpal and S. Hangirgekar, *Org. Biomol. Chem.*, **18**, 4575 (2020); https://doi.org/10.1039/D0OB00109K